# Analysis of Inlet Conditions in a CFD Application on Ester Immersed Power Transformers

Agustín Santisteban[1], Ramazan Altay[2], A. Kerem Köseoğlu[2], Alfredo Ortiz[1], Félix Ortiz[1], Fernando Delgado[1]

[1]*Departamento de Ingeniería Eléctrica y Energética. University of Cantabria*
*Av. los Castros s/n, 39005 Santander, Spain*
*agustin.santisteban@unican.es, alfredo.ortiz@unican.es ,felix.ortiz@unican.es, fernando.delgado@unican.es*
[2] *Balikesir Elektromekanik Sanayi Tesisleri Anonim Sirketi, BEST Transformers*
*10100 Balikesir, Turkey*
*ramazan.altay@besttransformer.com, kerem.koseoglu@besttransformer.com*

**Abstract.** This work presents a study of the cooling performance of a natural ester in a power transformer winding by using CFD analysis. Thus, the study is performed under heat-run test conditions and considers two different dielectric fluids, a mineral oil which is the original cooling fluid and a natural ester as an alternative fluid. The inlet boundary conditions are calculated by considering the thermal and hydraulic balance of the transformer cooling system. When considering natural ester, the inlet mass flow rate and temperature obtained are lower than the mineral oil case. For the CFD analysis, a portion of the low voltage winding in a 3D model is selected, using the Conjugate Heat Transfer model for the fluid-solid thermal interaction and the Boussinessq approach for the buoyancy terms. The results from transformer balance and thermal model obtained for mineral oil are compared to the heat run test results to validate the model. Regarding the CFD results, natural ester leads to higher hot-spot temperature in the winding and higher oil temperature rise than mineral oil.

**Keywords:** Computational fluid dynamics; Transformers; Cooling liquid

## 1 Introduction

Oil-immersed power transformers are one of the most expensive and critical components of an electrical system. Despite being highly efficient machines, a small fraction of the transferred power is lost in the form of heat (mainly in the windings), which must be removed. A heat-carrier dielectric fluid, generally a mineral oil, is used to remove the generated heat, and simultaneously provide electrical insulation. This liquid circulates around and through the windings cooling them, and thus preventing hot spots that negatively affects to the transformer lifetime. The dimensions of these cooling channels depend on the dielectric fluid properties, as well as the structural and electrical requirements, [1].

One of the most extended techniques for the thermal modelling of power transformers is the Computational Fluid Dynamics (CFD). In CFD, the governing principles of both fluid flow and heat transfer are written in the form of partial differential equations that are then replaced by algebraic equations and solved at discrete elements in time and space. During the last two decades, several authors have reported the CFD technique as a relevant tool to investigate and improve the thermal performance of power transformers windings. In the first decade, the main purpose of CFD was to determine the velocity and temperature profiles of a 2-D winding immersed in a mineral oil, [2–6]. More recently, the improvement of computational resources has enabled the use of 3-D models to conduct numerical investigations, allowing to capture three-dimensional phenomena that are impossible to find in 2-D models, [7–10]. These works model fluids and solids in the transformer, using the Conjugate Heat Transfer (CHT) model for the fluid-solid interface coupling.

More recent studies have been carried out using both 2-D and 3-D models to better understand and characterize the thermal-hydraulic performance of the insulation systems (oil and paper) with ester-based oils, as

well as to evaluate the cooling efficiency of several alternative liquids, [11–15]. Ester-based liquids overcome some disadvantages of mineral oils such as low flash and fire points as well as low biodegradability.

In this work, thermal modelling of a power transformer working under heat-run test conditions is carried out, using mineral oil and natural ester as cooling fluids, comparing the thermal performance of both fluids and considering a retrofilling scenario. For the CFD analysis, the inlet mass flow rate and temperature have been adjusted by doing a thermal and hydraulic balance of the cooling circuit.

# 2 CFD model

## 2.1 Geometry description

The geometry described on this section corresponds to the low voltage winding of a 100 MVA 154/33.6 kV ONAN power transformer that is currently manufactured by BEST Transformers. This study will focus on a detailed model of the low voltage winding to determine hot spots in the transformer. The studied winding is a layer winding with axial cooling ducts, as can be seen in Fig. 1.

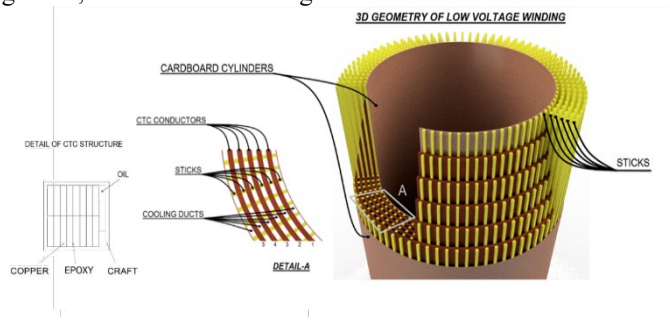


Fig. 1. Geometry and parts of the low voltage Winding and detail of CTC conductor.

The studied winding consists of an inner insulation cardboard cylinder of 784mm of diameter and five conductor layers, which are 16mm width. The spacers placed between layers form axial cooling ducts of 6mm width. 80 spacers are placed on the tangential direction, leading to 80 sectors of 4.5 degrees each. The geometry used for the model in this work is one of the 4.5-degree sectors of the winding, and since they are identical sections, there is no heat transfer from adjacent sections. For instance, symmetric/adiabatic boundary conditions can be applied on the section borders. The winding is formed by Continuously Transposed Conductor (CTC) with 16mm radial dimension and 15mm in axial dimension. The total height of the winding is 1634mm.

## 2.2 Governing equations

Regarding the CFD simulations, the solid and fluid interfaces inside the transformer winding are modelled using the Conjugate Heat Transfer model. Thus, different equations are considered for the fluid and solid domains. In the fluid domain, mass, momentum and energy conservation equations for a non-isothermal incompressible flow are considered. To model the buoyancy forces, the Boussinesq approach has been used in the model. For this approach, fluid properties are considered constant and calculated at the reference temperature. This model leads to the equations (1-3).

$$\nabla u = 0 \tag{1}$$

$$\rho \cdot \frac{\partial u}{\partial t} + \rho \cdot (u \cdot \nabla) u = -\nabla p + \mu(\nabla^2 u) + \rho_{ref} \cdot g \cdot \beta \cdot \left(T - T_{ref}\right) \tag{2}$$

$$\rho \cdot c_p \cdot \frac{\partial T}{\partial t} + \rho \cdot c_p \cdot \nabla \cdot (u\, T) = k \cdot \nabla^2 T \tag{3}$$

Where ρ is the fluid density, u is the velocity field, p is the pressure field, μ is the fluid viscosity, g is the gravity vector, β is the thermal expansion coefficient, $c_p$ is the specific heat of the fluid, k is the thermal conductivity of the fluid and T is the temperature field. In the solid domain, the temperature follows a diffusion

equation with a heat source representing the winding losses. Equation (4) describes the behavior of the temperature field inside the solid domain.

$$\rho\, c_p \frac{\partial T}{\partial t} = k \cdot \nabla^2 T + q_s \tag{4}$$

Where the term $q_s$ represents a volumetric heat source. The governing equations are solved using the Finite Volume Method (FMV) using the commercial software ANSYS Fluent and considering a steady-state study. For this problem, a structured hexahedral mesh is used for the FVM. Second Order Linear Upwind scheme is selected for the derivatives approach in a pressure-velocity coupled scheme of a pressure-based solver. The normalized residuals are set to be lower than $10^{-6}$, except for the energy equation residuals, that is set to be lower than $10^{-9}$. The final mesh consists of 7.4M elements, with 0.99 average orthogonal quality and 4e-3 average and 0.3 maximum skewness.

### 2.3 Boundary conditions

For the CFD modelling, it is important to set the adequate boundary conditions to the developed model. For this case, a velocity inlet condition was chosen, with uniform value of velocity for the momentum boundary condition and uniform temperature for the thermal boundary condition. The value of the inlet velocity and temperature are determined from the values obtained in the cooling circuit balance, which will be explained in the fourth section. At the outlet, a zero gauge pressure condition was set. External walls of the domain are considered as static walls with no-slip condition and adiabatic, since the thermal conductivity of the insulation cylinder is very low. This adiabatic condition has been used by other authors in their CFD model with good accuracy on their results [6][9]. Solid-fluid interface boundaries, such as disc walls, are considered as no-slip walls with thermal coupling (considered in the CHT model). For the heat losses, a volumetric heat source is considered in the conductor domain, which represents the losses under heat-run test conditions.

### 2.4 Material properties

***Dielectric fluid.*** Two different kinds of dielectric fluid are considered in this study. Mineral oils and natural esters will be considered for the cooling of the transformer windings. For the insulating fluids, the temperature dependent properties, with absolute temperature, are known and collected in Table 1. These equations are valid in the temperature range inside the transformer (from 303 to 373K).

Table 1. Temperature dependent properties of the fluids.

| | **Mineral oil** | **Natural ester** |
|---|---|---|
| **Density (kg/m$^3$)** | $1055.1 - 0.66 \cdot T$ | $1109.2 - 0.653 \cdot T$ |
| **Specific heat (J/kg·K)** | $1172.8 + 3.6097 \cdot T$ | $1273.15 + 1.952 \cdot T$ |
| **Conductivity (W/m$^2$·K)** | $0.1529 - 6.959e-5 \cdot T$ | $0.1317 + 4.142e-4 \cdot T - 8.86e-7 \cdot T^2$ |
| **Viscosity (Pa·s)** | $0.1271 - 6.39754e-4 \cdot T + 8.1502e-7 \cdot T^2$ | $7.99 - 6.63e-2 \cdot T + 1.84e-4 \cdot T^2 - 1.71e-7 \cdot T^3$ |
| **Thermal expansión coefficient (1/K)** | 6.26e-4 | 5.89e-4 |

The density of both fluids shows a linear dependence on temperature, which corresponds to a constant thermal expansion coefficient that is used in the Boussinesq model. To calculate the reference properties for the fluids, the previous formulae are used for the reference temperature of each model, which is the bottom oil temperature in the transformer.

***Solid material properties.*** In order to reduce the complexity of the geometry of the CTC winding conductors and saving computational resources, an equivalent material is chosen that represents the behavior of the real conductor. This methodology has also been implemented by other authors [12]. Thus, an equivalent thermal conductivity that represents the global heat transfer mechanism of the CTC conductors is calculated. For the model, an orthotropic thermal conductivity on cylindrical coordinates is selected, using values of 0.72, 1.27 and 385 W/m·K for radial,

axial and tangential thermal conductivity, respectively.

# 3 Calculation of inlet conditions

This section describes the methodology followed to estimate the values of the mass flow and temperatures of the oil through the transformer windings, which will be the inlet conditions in a subsequent CFD analysis. By doing this, the boundary conditions can be suited for a retrofilling scenario of transformers with an alternative liquid. This methodology leads to different mass flow and temperatures at the inlet for different fluids. The methodology for the cooling circuit balance is based on the transformer equilibrium described in [16].

Due to the complexity of the High Voltage Winding cooling system, the temperature rise on this winding is considered the same as the Low Voltage Winding. It is also assumed that all the mass flow through the windings goes to the radiators, considering negligible the mass flow in other parts of the tank.

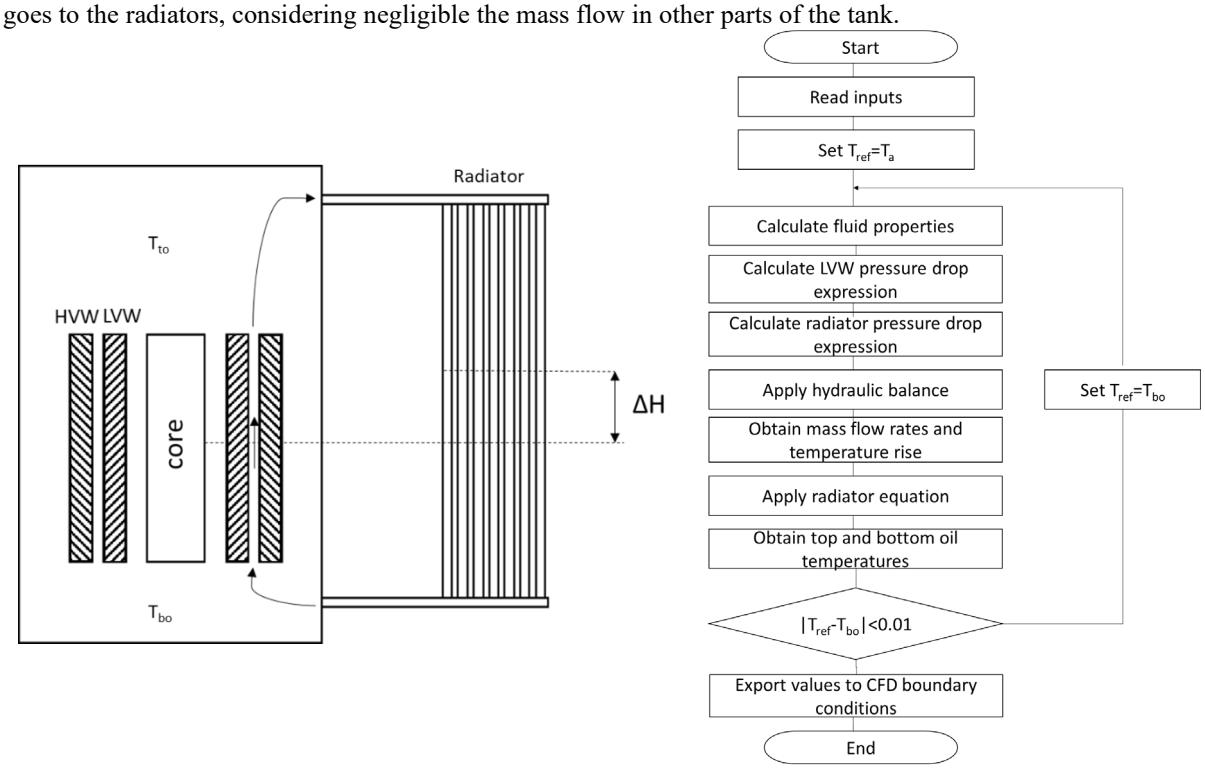


Fig.2. Scheme of the transformer cooling circuit

Fig.2 represents the schematic view of the transformer, representing the main components of the cooling circuit, the windings and radiators. The insulating oil flows through winding driven by natural convection. The oil enters the winding at bottom oil temperature. After that, the oil flows through radiators where its temperature decreases from top oil temperature ($T_{to}$) to bottom oil temperature ($T_{bo}$). Convective and radiative heat exchange mechanisms cool down the insulating oil flowing through the radiators. These heat exchange mechanisms in the radiators are represented by a global heat transfer coefficient. For the study of the radiator, an average radiator is selected, that dissipated the proportional part of the heat losses inside the transformer and its behavior represents all radiators of the cooling system.

For the calculations, the core losses are neglected since the input data comes from heat run test. This means that all the heat losses are located in LVW and HVW during the transformer test

Table 2. Mass flow rates and temperatures obtained with the methodology proposed.

| | **Mineral oil** | **Natural ester** |
|---|---|---|
| **$m_{lvw}$ (kg/s)** | 0.748 | 0.396 |
| **$m_{hvw}$ (kg/s)** | 1.185 | 0.629 |

| | | |
|---|---|---|
| **ΔT (K)** | 16.3 | 38.2 |
| **$T_{bo}$ (K)** | 338 | 329.3 |
| **$T_{to}$ (K)** | 354.3 | 367.5 |

Table 2 shows the values obtained for the mass flow rates and temperatures using the methodology previously described when considering mineral oil and natural ester as cooling fluids. It can be appreciated that the mass flow rate is reduced when considering natural ester as cooling fluid due to the higher viscosity of this fluid. Lower mass flow rates lead to higher oil temperature rise in the transformer and higher thermal driving pressure. Regarding the bottom oil temperature, natural ester case is 9K lower than the case of mineral oil.

# 4 CFD Results and discussion

## 4.1 Previous studies

The first preliminary study is a mesh independence test. The objective of the test is to compare the results obtained from each mesh to check that the mesh has no influence over the CFD results. With the three different meshes tested, from a coarse to a fine mesh, the results obtained have shown small variations, less than 1K regarding the maximum temperatures, using the intermediate mesh as reference. In addition, an uncertainty analysis has been performed, obtaining less than 1% of uncertainty on the temperature rise for the selected mesh.

The second preliminary study is a validation of the results obtained in the calculation of the inlet condition, described in section 3, and the CFD simulations, comparing the results obtained with the heat run test performed in the transformer. The test followed the standard IEC60076-2011-02 and fiber optic (FO) probes were used for temperature measurements of the winding, top oil, and bottom oil. Regarding the cooling circuit balance, all the calculations have been carried out considering the mineral oil, which was used in the heat run test. Later, the values of the top and bottom oil temperatures, located at the inlet and outlet of transformer radiators, obtained from the methodology proposed are compared with the test values in Table 3.The results shows small deviations between calculated and experimental values for bottom-oil and top-oil temperatures, being these deviations lower than 0.2K.

Table 3.Comparison between calculated and experimental results.

| | **Calculated value** | **Experimental test** |
|---|---|---|
| **$m_{lvw}$ (kg/s)** | 0.748 | - |
| **$m_{hvw}$ (kg/s)** | 1.185 | - |
| **ΔT (K)** | 16.3 | 16.45 |
| **$T_{bo}$ (K)** | 338 | 337.9 |
| **$T_{to}$ (K)** | 354.3 | 354.4 |

The detailed CFD winding model is also compared with experimental values of the test. FO probes are located in the fourth layer of the low voltage winding, at different tangential position, and positioned 100m below the top part of the winding. The temperature from these probes has been compared with the obtained from CFD simulations in the probes position, obtaining a 1.8K deviation between the CFD and experimental results.

## 4.2 Results and discussion

Regarding the CFD results, the winding temperature increases with height, obtaining the hottest locations on the top part of each layer, as can be seen in Fig. 3. In addition, it can be appreciated that the exterior layers show lower temperatures than the interior. This effect is led by the fact that the external oil ducts are heated only from one side, having lower local temperatures, and leading to better cooling, as shown in Fig. 3, where the highest temperatures are observed in the internal layers.

Fig. 3 shows the evolution of the winding temperature along the winding height. At the beginning, a fast increase of temperature is caused by border effect. Then there is a region where the temperature increases in a nonlinear trend. In this region, the flow is thermally developing. After this region, the temperature increases in a linear trend. In that region the flow is thermally fully developed, and the heat transfer rate is constant, leading to

the linear trend of temperature rise. At the top part of the winding, a fast decrease of temperature is caused by border effect.

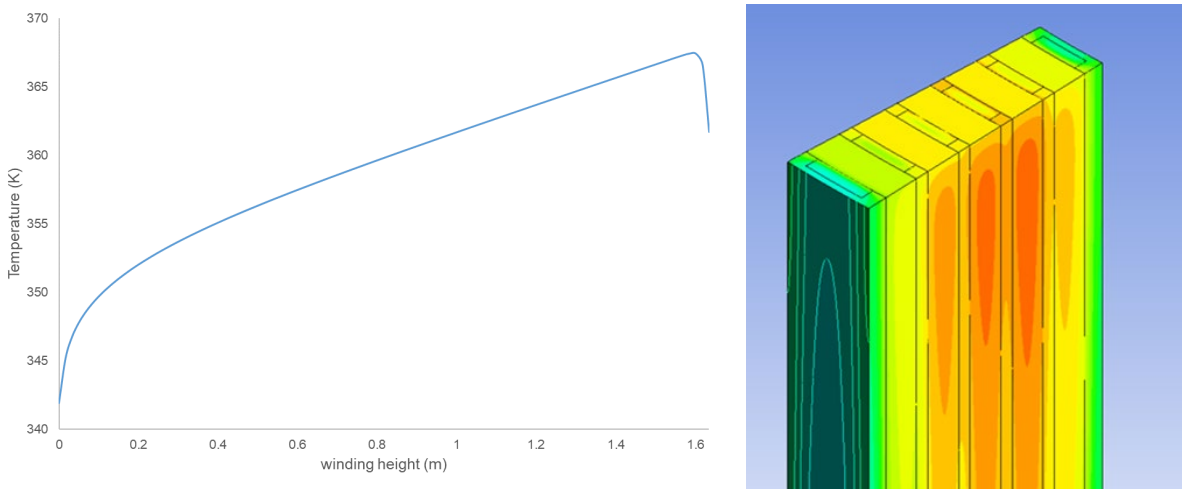


Fig.3. Temperature distribution in the low voltage winding with mineral oil.

For natural ester, similar temperature increase in the axial direction is observed, but the temperature rise is higher than for the mineral oil. The lower mass flow rate leads to higher winding and hot spot temperatures ($T_{hs}$), as can be seen in Table 4.

Table 4. Comparison of mass flow and temperature between both liquids.

| | **Mineral oil** | **Natural ester** |
|---|---|---|
| **$m_{lvw}$ (kg/s)** | 0.748 | 0.396 |
| **$T_{bo}$ (K)** | 338 | 329.3 |
| **$T_{hs}$ (K)** | 370.5 | 385.7 |

From the cooling circuit balance results can be observed that for the natural ester, since the viscosity is higher than mineral oil, the pressure drop in transformer components, such as windings or radiators, is higher. This leads to a reduction on the mass flow rate of the natural ester, which makes the temperature rise and the thermal driving pressure increase. The total mass flow rate through windings with natural ester is reduced to be the 53% of the total mass flow rate for mineral oil.

Regarding the top and bottom oil temperatures, the reduction of mass flow rate leads to a higher bottom to top oil temperature rise for natural ester and a higher top oil temperature. This leads to higher oil to ambient temperature gradient, which means a reduction of the bottom oil temperature with respect to the mineral oil case. The bottom oil temperature is 8.7 K lower and the top oil temperature is 13.2K higher in the natural ester case.

It can be appreciated that natural ester leads to higher winding temperatures, mainly caused by the lower mass flow rate through the winding. In Fig 3 it can be appreciated that the exterior layers, most internal and most external, show lower temperature due to the first and last duct are heated only by one side. In this case, the natural ester case predicts a hot-spot temperature 15.7 K higher than the mineral oil. In both cases, the hot spot is located in the second layer of the winding.

## 5 Conclusions

In this work, the thermal modelling of a low voltage winding of a 100 MVA power transformer working under heat run test conditions has been performed. Two different fluids have been considered in a detailed winding CFD model, a mineral oil and a natural ester. The mass flow rate and inlet temperature were calculated from the hydraulic and thermal balance of the transformer cooling circuit, obtaining the inlet conditions for the CFD simulations.

From the cooling circuit balance with mineral oil and natural ester, the mass flow rate with the ester is reduced due to fluid viscosity. The high viscosity leads to lower mass flow rate and bottom oil temperature in case of oil natural flow. Higher temperature rise is also obtained in the case of the ester-based fluid.

Regarding the winding model, both fluids show similar temperature distribution and similar hydraulic behavior. The main difference is the thermal entrance length, caused by different Reynolds number at the inlet. With respect to the cooling performance, natural ester leads to higher hot spot temperature in the winding.

In general, this work has shown that, when comparing the performance of an ester-based fluid and a mineral oil inside a power transformer winding, the ester based-fluid leads to higher temperatures. In a retrofilling scenario, it is important to consider the complete cooling circuit in order to estimate the proportion of mass flow rate when using a new fluid with higher viscosity for the comparison. This work has showed that the higher viscosity affects more negatively the cooling performance of the natural ester, even if the thermal properties, such as thermal conductivity and specific heat, are higher.

**Acknowledgment.** This work has received funding, in the framework of the BIOTRAFO project, from the European Union's Horizon 2020 research and innovation program under the Marie Sklodowska-Curie grant H2020-MSCA-RISE-2018- 823969, 2019-21. In addition, the work has received financial support of the Spanish Ministry of Science and Innovation by means of the National Research Project PID2019-107126RB-C22.

**Authorship statement.** The authors hereby confirm that they are the sole liable persons responsible for the authorship of this work, and that all material that has been herein included as part of the present paper is either the property (and authorship) of the authors, or has the permission of the owners to be included here.

## References

[1] "Electrical Insulating Oils," in ASTM Special Technical Publication, 1988.
[2] J. M. Mufuta and E. Van Den Bulck, "Modelling of the mixed convection in the windings of a disc-type power transformer," Appl. Therm. Eng., vol. 20, no. 5, pp. 417–437, 2000.
[3] N. El Wakil, N.-C. Chereches, and J. Padet, "Numerical study of heat transfer and fluid flow in a power transformer," Int. J. Therm. Sci., vol. 45, no. 6, pp. 615–626, 2006.
[4] J. Smolka, O. Bíró, and A. J. Nowak, "Numerical simulation and experimental validation of coupled flow, heat transfer and electromagnetic problems in electrical transformers," Arch. Comput. Methods Eng., vol. 16, no. 3, pp. 319–355, 2009.
[5] F. Torriano, M. Chaaban, and P. Picher, "Numerical study of parameters affecting the temperature distribution in a disc-type transformer winding," Appl. Therm. Eng., vol. 30, no. 14–15, pp. 2034–2044, 2010.
[6] A. Skillen, A. Revell, H. Iacovides, and W. Wu, "Numerical prediction of local hot-spot phenomena in transformer windings," Appl. Therm. Eng., vol. 36, no. 1, pp. 96–105, 2012.
[7] F. Torriano, P. Picher, and M. Chaaban, "Numerical investigation of 3D flow and thermal effects in a disc-type transformer winding," Appl. Therm. Eng., vol. 40, pp. 121–131, 2012.
[8] M. A. Tsili, E. I. Amoiralis, A. G. Kladas, and A. T. Souflaris, "Power transformer thermal analysis by using an advanced coupled 3D heat transfer and fluid flow FEM model," Int. J. Therm. Sci., vol. 53, pp. 188–201, 2012.
[9] F. Torriano, H. Campelo, M. Quintela, P. Labbé, and P. Picher, "Numerical and experimental thermofluid investigation of different disc-type power transformer winding arrangements," Int. J. Heat Fluid Flow, vol. 69, no. November 2017, pp. 62–72, 2018.
[10] M. Quintela, H. Campelo, F. Torriano, P. Labbé, and P. Picher, "Assumptions and Numerical Parameters Influencing the Accuracy of Thermal Models for Core-Type Power Transformer," no. August 2017.
[11] I. Fernández et al., "Thermal degradation assessment of Kraft paper in power transformers insulated with natural esters," Appl. Therm. Eng., vol. 104, 2016.
[12] T. W. Park and S. H. Han, "Numerical analysis of local hot-spot temperatures in transformer windings by using alternative dielectric fluids," Electr. Eng., vol. 97, no. 4, pp. 261–268, 2015.
[13] R. C. Breazeal, A. Sbravati and D. M. Robalino, "Evaluation of Natural Ester Retrofilled Transformers After One Year of Continuous Overload," 2019 IEEE Electrical Insulation Conference (EIC), Calgary, AB, Canada, 2019, pp. 115-119, doi: 10.1109/EIC43217.2019.9046617.
[14] A. Santisteban, A. Piquero, F. Ortiz, F. Delgado, and A. Ortiz, "Thermal Modelling of a Power Transformer Disc Type Winding Immersed in Mineral and Ester-Based Oils Using Network Models and CFD," IEEE Access, vol. 7, pp. 174651–174661, 2019.
[15] X. Zhang, Z. Wang, Q. Liu, M. Negro, A. Gyore, and P. W. R. Smith, "Numerical investigation of influences of liquid types on flow distribution and temperature distribution in disc type ON cooled transformers," 2017 IEEE 19th Int. Conf. Dielectr. Liq. ICDL 2017, vol. 2017–Janua, no. Icdl, pp. 1–4, 2017.
[16] Z. R. Radakovic and M. S. Sorgic, "Basics of detailed thermal-hydraulic model for thermal design of oil power transformers," IEEE Trans. Power Deliv., vol. 25, no. 2, pp. 790–802, 2010.